

An Enhanced DTC scheme for Induction Machine Control Fed by Seven-Level MPC Voltage Source Inverter

O.Chandra sekhar¹ K.Chandra sekhar² G. Durga Sukumar³

¹ Professor, E.E.E Department, Koneru Lakshmaiah University, Vaddeswaram, sekhar.obbu@gmail.com

² Professor, E.E.E Department, R.V.R & J.C College of Engg, Chowdavaram, Guntur, India, cskoritala@gmail.com

³ E.E.E Department, Vignan University, Vadlamudi, India, gdurgasukumar@gmail.com

Abstract: A novel multilevel control structure for induction motor based on the Direct Torque Control (DTC) strategy using a seven-level Multi Point Clamped (MPC) Voltage Source Inverter (VSI) is presented. It is shown that the multilevel topology presents enough degrees of freedom to control both electromagnetic torque and stator flux with very low ripple and high dynamics on other side. Simulation results, obtained with two-level, three-level inverter, five-level and with seven-level inverter, are presented and compared. This analysis shows that feeding electrical drive with multi level inverter can greatly improves the drive performance. The performance of this control method has been demonstrated by simulations performed using a versatile simulation package, Matlab/Simulink.

Key words: DTC, seven-level MPC VSI, Induction motor, Matlab/Simlink.

1. Introduction

Multilevel power conversion technology is a very rapid growing area of power electronics with good potential for further development. The most attractive application of this technology are in the medium to high voltage range (2-13kv), and include induction motor drives, power distribution, power quality and power conditioning applications [1],[2],[3]. In general multilevel power converters can be viewed as voltage synthesizers, in which the high output voltage is synthesized from many discrete small voltage levels. The main advantages of this approach is, The voltage capacity of the existing devices can be increased many times without the complications of static and dynamic voltage sharing that occurring series connected device. It is possible to obtain refined voltage wave forms and reduced THD in voltage with increased number of voltage levels. It is possible to reduce the electromagnetic interference problem by reducing the switching dv/dt stress. Multilevel wave forms naturally limit the problems of large voltage transients that occur due to the reflections on cables, which can damage the motor windings and cause other problems.

The diode-clamped multilevel converter employs clamping diodes and series DC capacitors to produce AC Voltage waveforms with multiple levels, [4], [5],[6],[7]. The converter can be generally configured as a multilevel topology, but only the three-level converter, also referred as Multi Point Clamped (MPC) converter, has found wide application in medium-voltage high-power applications [8],[9]. The main features of the MPC converter include reduced dv/dt and Total Harmonic Distortion (THD) in its AC output voltages in comparison to the conventional two level converters. As in any multilevel converter it can be used in the medium-voltage applications to reach a certain voltage level without series connection of power semiconductors.

The three prominent multilevel inverters topologies can be used in motor drive applications. Cascaded multilevel inverters are well suited for applications where several dc power supplies could be available, such as in automotive applications. Diode-clamped and flying-capacitor multilevel structures are well suited for drives directly connected to the utility power system in the high- and medium-voltage ranges. Due to the advantage of needing only one power supply, inverters based in these topologies are very attractive for industrial Variable-Speed Drive (VSD) applications.

When diode-clamped or flying-capacitor multilevel-based inverters are used in VSD applications, the voltage across the capacitors used in these topologies could diverge from its required value [10], [11], [12], [13], [14], [15]. The control strategy used to command the multilevel inverter must take into account the charging and discharging phenomena of the capacitors.

In principle, DTC method is based on instantaneous space vector theory. By optimal selection of the space voltage vectors in each sampling period, DTC achieves effective control of the electromagnetic torque and the stator flux on the basis of the errors between their references and estimated values. It is possible to directly control the inverter states through a switching table, in order to reduce the torque and flux errors within the desired bands limits [16],[17]. The present work is based on the study of the application of DTC to the seven-level MPC VSI.

2. Proposed Seven-level Inverter Topology

Important technological improvements have been achieved in the design of fast full-controlled semiconductors like IGBTs. These improvements have allowed the increase of maximum voltage and current ratings, but an important limitation on the handled power still exists. Besides, the use of IGBTs with fast

switching under high voltages may generate high dV/dts, which may increase Electromagnetic interference and windings insulation stress. In order to overcome these drawbacks an evolution toward new and more efficient conversion structures, such as multilevel inverters, has been observed in the field of medium voltage drive applications (up to 6.6 kV rated motors).

Table 1: Switching states of a Seven-level inverter

<i>Switches state</i>										<i>Output Voltage (V_{AO})</i>
S_{a1}	S_{a2}	S_{a3}	S_{a4}	S_{a5}	S_{a6}	S_{a7}	S_{a8}	S_{a9}	S_{a10}	
<i>ON</i>	<i>OFF</i>	<i>OFF</i>	<i>ON</i>	<i>OFF</i>	<i>ON</i>	<i>OFF</i>	<i>OFF</i>	<i>OFF</i>	<i>OFF</i>	$-3U_0$
<i>OFF</i>	<i>ON</i>	<i>ON</i>	<i>ON</i>	<i>OFF</i>	<i>OFF</i>	<i>OFF</i>	<i>OFF</i>	<i>OFF</i>	<i>OFF</i>	$-2U_0$
<i>OFF</i>	<i>OFF</i>	<i>ON</i>	<i>ON</i>	<i>OFF</i>	<i>OFF</i>	<i>OFF</i>	<i>ON</i>	<i>OFF</i>	<i>OFF</i>	$-U_0$
<i>OFF</i>	<i>OFF</i>	<i>OFF</i>	<i>OFF</i>	<i>ON</i>	<i>ON</i>	<i>OFF</i>	<i>OFF</i>	<i>ON</i>	<i>ON</i>	0
<i>OFF</i>	<i>OFF</i>	<i>ON</i>	<i>OFF</i>	<i>OFF</i>	<i>OFF</i>	<i>OFF</i>	<i>ON</i>	<i>OFF</i>	<i>OFF</i>	0
<i>OFF</i>	<i>OFF</i>	<i>OFF</i>	<i>OFF</i>	<i>ON</i>	<i>ON</i>	<i>ON</i>	<i>OFF</i>	<i>OFF</i>	<i>OFF</i>	U_0
<i>OFF</i>	<i>OFF</i>	<i>ON</i>	<i>ON</i>	<i>ON</i>	<i>ON</i>	<i>OFF</i>	<i>OFF</i>	<i>OFF</i>	<i>OFF</i>	$2U_0$
<i>OFF</i>	<i>OFF</i>	<i>OFF</i>	<i>OFF</i>	<i>ON</i>	<i>ON</i>	<i>ON</i>	<i>OFF</i>	<i>OFF</i>	<i>OFF</i>	$3U_0$

Table 2: Seven-level inverter output magnitudes of space voltages vectors

<i>Group</i>	<i>Magnitude of Voltage Vectors</i>
<i>1</i>	$[V_0],$
<i>2</i>	$[V_1, V_2, V_3, V_4, V_5, V_6],$
<i>3</i>	$[V_{44}, V_{45}, V_{46}, V_{47}, V_{48}, V_{49}],$
<i>4</i>	$[V_{63}, V_{64}, V_{65}, V_{66}, V_{67}, V_{68}],$
<i>5</i>	$[V_{75}, V_{77}, V_{79}, V_{81}, V_{83}, V_{85}],$
<i>6</i>	$[V_{100}, V_{101}, V_{102}, V_{103}, V_{104}, V_{105}, V_{106}, V_{108}, V_{110}, V_{112}, V_{113}, V_{114}, V_{115}, V_{116}, V_{117}, V_{118}, V_{125}],$
<i>7</i>	$[V_{205}, V_{206}, V_{207}, V_{208}, V_{209}, V_{210}],$
<i>8</i>	$[V_{218}, V_{219}, V_{220}, V_{221}, V_{222}, V_{223}, V_{224}, V_{225}, V_{226}, V_{228}, V_{230}, V_{232}, V_{234}, V_{236}, V_{237}],$
<i>9</i>	$[V_{296}, V_{297}, V_{298}, V_{299}, V_{300}, V_{301}, V_{302}, V_{303}, V_{304}, V_{305}, V_{306}, V_{308}, V_{310}, V_{312}, V_{314}, V_{316}],$

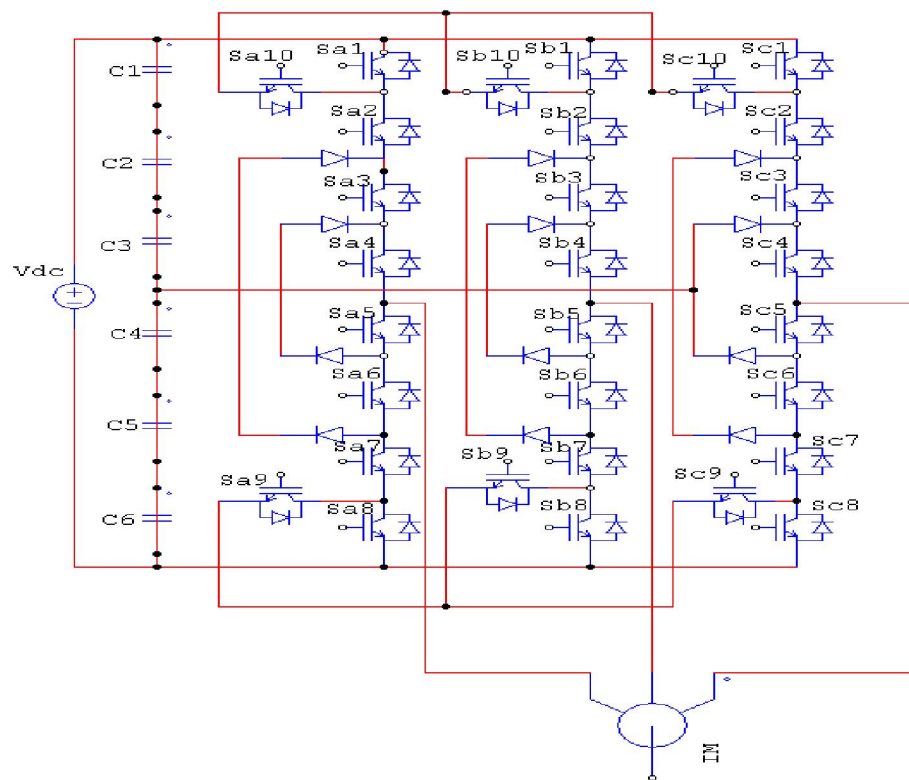


Fig.1: Proposed Seven-level MPC VSI topology

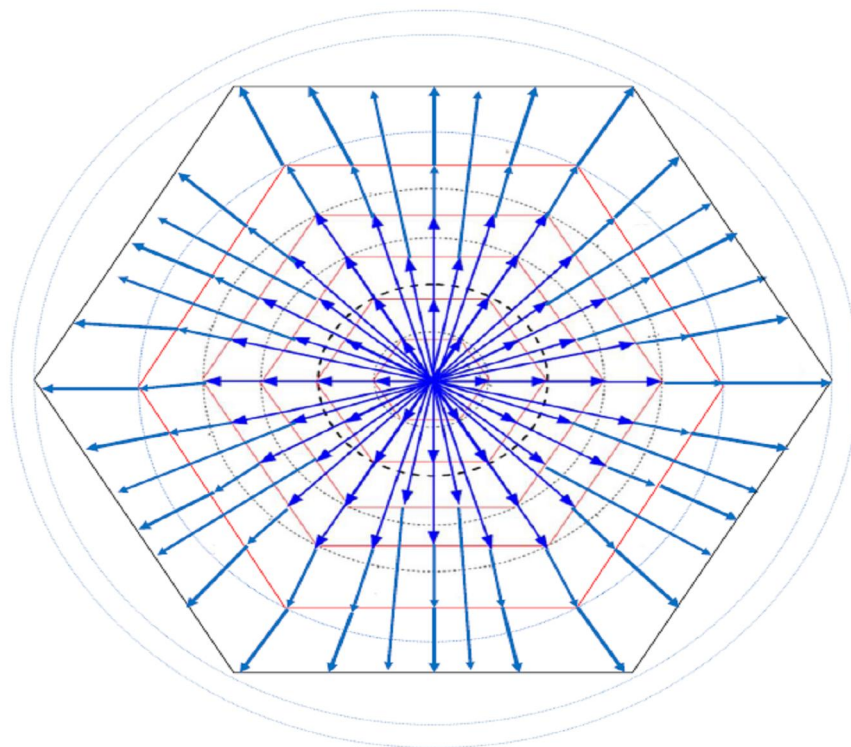


Fig.2: Space Vector diagram of Seven-level Inverter

Fig.1 shows the schematic diagram of Multi Point Clamped (MPC) seven-level VSI. Each phase consists of eight switches, each of which with a freewheeling diode in series and two other in parallel and two clamping diodes that allow the connection of the phases outputs to the middle point O. Table 1 illustrates the switching states of proposed inverter for one phase.

Seven-level MPC converter topology typically consists of six capacitors on the DC bus and seven levels of the phase voltage. Fig.1 shows a seven-level MPC inverter topology in which the DC bus consists of six capacitors C_1, C_2, C_3, C_4, C_5 and C_6 . For V_{dc} , DC bus voltage, the voltage across each capacitor is $V_{dc}/6$, with its device voltage stress restricted to one capacitor voltage level $V_{dc}/6$, with the help of clamping diodes.

Fig.2 shows the Seven-level inverter has 343 switching states and there are 78 effective vectors. According to the magnitude of the voltage vectors, we divide them into nine groups as shown in table 2.

3. SVM Algorithm Implementation of Seven-Level Inverter

A qualitative space vector pulse width modulation algorithm for multi point clamped multilevel inverter is presented. In this method, the duty cycles of reference voltage vectors are exacted accordingly for recognizing the position of the reference voltage vector in each region. The suitable switching sequence of the region and calculation of the switching ON times for each state is estimated. The same system can be applied even to high-level inverters.

The sector identification can be done by using coordinate alteration of the reference vector into a two dimensional coordinate system. However, the sector can also be identified with the help of its reference phase vector along a, b and c axis and by periodic contrast with the discrete phase voltages. After identifying the sector, the voltage vectors at the vertices of the sector are to be determined. Once the switching voltage space vectors are determined the switching sequences can be identified using lookup tables. The calculations of the duration of the voltage vectors can be simplified by mapping the identified sector corresponding to a sector of two-level inverter. To obtain optimum switching, the voltage vectors are to be swapped for their respective durations, in a sequence such that only one switching follows as the inverter transfers from one switching state to another.

The duty cycles of reference voltage vector will be m_1, m_2 and $1 - (m_1 + m_2)$. The values of m_1 and m_2 come handy in identifying the region where reference vector is located, which is the major problem in case of multilevel inverters.

This method presents an improvement to the duty cycles of reference vector applied to spot the location of reference vector easily in each of the regions of a multilevel inverter. Once the region is identified, the

appropriate switching sequence of the region can be identified. The ON time period for each state can be calculated with the obtained duty cycles.

The space vector V_s constituted by the pole voltages;

V_{AO}, V_{BO} and V_{CO} is defined as:

$$\mathbf{V}_{ref} = V_{AO} + V_{BO} \exp[j(2\pi/3)] + V_{CO} \exp[j(4\pi/3)] \quad (1)$$

The dwelling time periods T_1, T_2 and T_0 are

$$T_1 = \frac{|\mathbf{V}_{ref}| T_s \sin(\pi/3 - \alpha)}{V_{dc} \sin(\pi/3)}$$

$$T_2 = \frac{|\mathbf{V}_{ref}| T_s \sin \alpha}{V_{dc} \sin(\pi/3)}$$

$$T_0 = T_s - (T_1 + T_2) \quad (2)$$

In multilevel inverters, the reference voltage vector can be reproduced in the average sense by switching amongst the inverter states situated at the vertices, which are in a closest proximity to it. In case of a two-level inverter, the recognition of a reference vector is directly identified of its location in a sector. However, in higher level inverter; the presence of more than one region in a sector requires additional mathematical computation to recognize the region where the reference vector is located. The duty cycles (ON time for each state) will be found by equating volt-seconds of reference voltage with the closest three states.

$$m = d_1 V_1 + d_2 V_2 + d_3 V_3 \quad (3)$$

Where d_1, d_2 and d_3 are duty cycles of the nearest voltage vectors V_1, V_2 and V_3 and 'm' is the voltage reference vector.

3.1 Duty Cycles Calculation

The vector states at vertices of each region can be identified from space vector diagrams. The space vector diagram of sector-I of a Seven-level inverter is shown in Fig.3.

The reference vector m_3 is positioned in region 2 of three-level inverter. The m_6 and m_7 are reference vectors positioned in region 21 of a six-level inverter and in region 29 of a seven-level inverter respectively. m_{x1} and m_{x2} ($x=3$ or 6 or 7) are projections of reference vectors with reference to zero axis and sixty degrees axis ('q' is the angle made by reference vector from zero axis i.e., starting of sector 1; be noted m_3, m_6 and m_7 have different angle 'q' values).

The reference vector can be synthesized by sequential switching of nearest three switching states (vertices of the region wherein reference vector is present).

The lengths of new vectors can be found using the equations as

$$m_1 = m \times (\cos\theta - \sin\theta / \sqrt{3})$$

$$m_2 = 2 \times m \times (\sin\theta / \sqrt{3}) \quad (4)$$

The values of m_1 and m_2 for reference vector in each region can be calculated with Eq. (4). The duty cycles of vertices of reference voltage will be m_1 , m_2 and $[1-(m_1+m_2)]$. For example, with reference to m_3 (reference vector in region 2), the reference vector can be synthesized by switching vectors V_1 , V_2 and V_3 . It will be important to note that duty cycle for switching state V_1 shall be nonetheless length of the vector joining V_3 and V_1 , whereas, m_1 is the projection of reference vector m_3 from the origin. As such, the corrected duty cycle for switching state V_1 in present case would be $(m_1-0.167)$. The length of vector joining V_1 and V_2 is m_2 . As such, corrected duty cycles for switching states V_1 , V_2 and V_3 would be $(m_1-0.167)$, m_2 and $(0.833-m_1-m_2)$ respectively. The values of m_1 and m_2 are useful in identifying the region where reference vector is located, which is the major problem in multilevel inverters. Once the region is identified, the appropriate switching sequence of that region can be identified. The ON time period for each state can be calculated by the duty cycles obtained:

$$\begin{aligned} T_{ON} \text{ for state1} &= T_s \times m_1 \\ T_{ON} \text{ for state2} &= T_s \times m_2 \\ T_{ON} \text{ for state3} &= T_s \times [1 - (m_1+m_2)] \end{aligned} \quad (5)$$

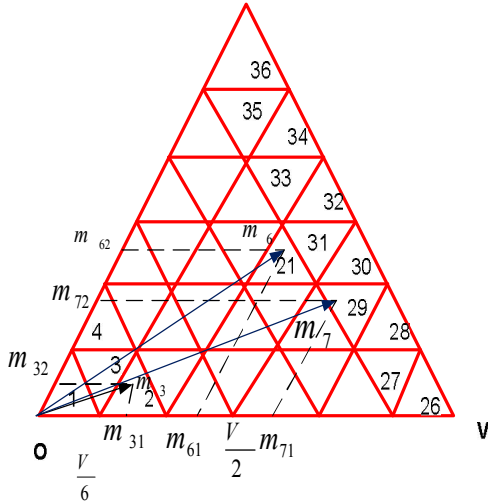


Fig. 3: Sector-I of seven-level inverter

4. Proposed Direct Torque Control using Seven- level MPC Inverter fed VSI

When a Seven-level inverter is used to feed DTC induction motor, the number of available space voltage vectors is increased, as the number of discrete voltage levels per phase is increased. A typical block diagram of a seven-level MPC inverter feeding DTC induction motor drive is shown in Fig.4. The IM control strategy will generate a space voltage vector requirement in order to keep the given external references (torque, speed or position) at their right values. The inverter control

strategy must command each inverter leg with the voltage level needed to have the requested voltage vector.

In a symmetrical three-phase induction machine, the instantaneous electromagnetic torque is given by

$$T = \frac{3}{2} p \vec{i}_s \cdot j \vec{\Psi}_s \quad (6)$$

Where $\vec{\Psi}_s$ is the stator-flux-linkage vector, \vec{i}_s is the stator current vector, and the 'p' number of pole pairs.

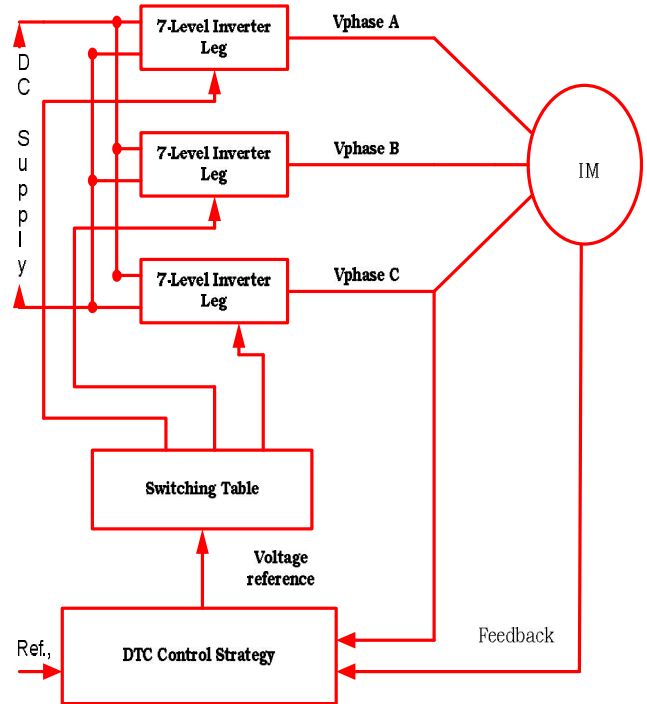


Fig.4: Proposed Block diagram of 7-level MPC inverter DTC IM drive

Both space vectors are expressed in the stationary reference frame. Another equivalent expression to calculate the electromagnetic torque, which gives an extremely clear idea of the process of controlling torque in a DTC system, is as follows.

The electromagnetic torque given by equation (7) is a sinusoidal function γ of, the angle between $\vec{\Psi}_s^s$ and $\vec{\Psi}_r^r$ as shown in Fig. 5.

Since the rotor flux changes slowly, the rapid variation of stator flux space vector will produce a variation in the developed torque because of the variation of the angle γ between the two vectors:

$$\Delta T_e = \frac{3}{2} \cdot \frac{P}{2} \cdot \frac{L_m}{L_s L_r - L_m^2} \left[\left(\vec{\Psi}_s^s + \Delta \vec{\Psi}_s^s \right) j \vec{\Psi}_r^r \right] \quad (7)$$

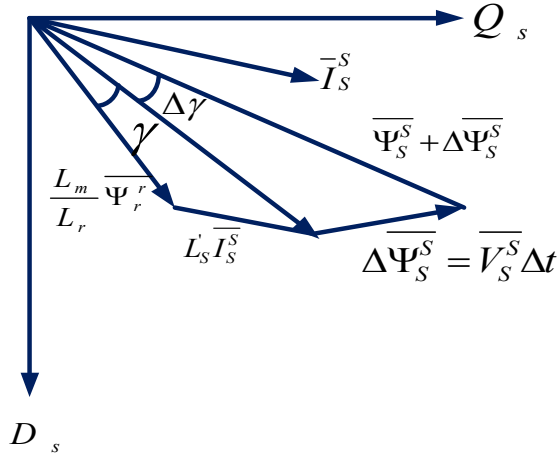


Fig.5: Induction motor flux phasor diagram

Therefore, to obtain a good dynamic performance, an appropriate inverter voltage vectors \bar{V}_i has to be selected to obtain stronger rotation speed of The actual value of stator flux can be expressed as ω_s The actual value of stator flux can be expressed as

$$\bar{\Psi}_s^s = \int (\bar{V}_s^s - \bar{i}_s^s R_s) dt \quad (8)$$

Where \bar{V}_s^s and \bar{i}_s^s indicate the measured stator voltage and current respectively.

The electromagnetic torque is calculated by means of equation (9)

$$T_e = \frac{3}{2} \cdot P \cdot (\Psi_{ds}^s i_{qs}^s - \Psi_{qs}^s i_{ds}^s) \quad (9)$$

On the other hand, the stator voltage space vector is given by

$$\bar{V}_s = R_s * \bar{i}_s + \frac{d}{dt} \bar{\Psi}_s \quad (10)$$

Where R_s is the stator resistance. If it is assumed that the stator ohmic drops can be neglected, then

$$\bar{V}_s = \frac{d\bar{\Psi}_s^s}{dt} \quad (11)$$

which simply means that the stator voltage directly defines the stator flux and, thus, the required stator flux locus will be obtained by using the appropriate inverter voltage vector. By assuming a slow motion of the rotor-flux-linkage space vector, if a stator voltage space vector is applied, which causes a quick movement of the stator flux linkage vector, then the electromagnetic torque will be increased. This is because the angle γ is increased. However, if a voltage space vector is applied which almost stop the rotation of the stator-flux-linkage space vector, then the electromagnetic torque will be decreased, because the rotor-flux-linkage vector is still

moving and the angle γ decreases

Therefore the variation of the stator flux space vector due to the application of the stator voltage vector \bar{V}_s^s during a time interval of Δt can be approximated as

$$\Delta\bar{\Psi}_s^s = \bar{V}_s^s \Delta t \quad (12)$$

As in the original DTC principle [18], [19],[20] the $\alpha - \beta$ plane will be divided into several sectors. In a multilevel inverter the number of available discrete voltage vectors is more important than those obtained with a two-level inverter. Thus, the $\alpha - \beta$ plane will be divided into 12 sectors rather than six, at each one of these sectors, an appropriate voltage vector will be assigned to keep flux and torque references as needed. For the switching vector selection, it is necessary to known the angular sector in which the actual flux is located. The actual position of the stator flux can be determined by equation (13), from the orthogonal flux components:

$$\alpha = \angle \bar{\Psi}_s^s = \tan^{-1} \left(\frac{\Psi_{qs}^s}{\Psi_{ds}^s} \right) \quad (13)$$

The selection of the appropriate voltage vector is based on the switching table given in Table 3. The input quantities are the stator flux sector and the outputs of the two hysteresis comparators. The flux control is made by classical two-level hysteresis controller, so a high level performance torque control is required, and the torque is controlled by an hysteresis controller built with six lower bounds and six upper known bounds.

Positive torque is applied for acceleration and negative torque is applied for retardation. When controlled torque reaches the positive lower hysteresis band, the full voltage vector is replaced with half voltage. If torque increases beyond the positive upper torque band, the zero voltage vectors are applied to decrease the developed torque. For reverse rotation, in the same way, retarding voltage vectors are applied.

A combination of the controller's outputs and the sector is then applied to a new optimal switching table (Table 3) which will give the appropriate voltage vector to reduce the number of commutation and the level of steady state ripple

5. Simulation Results and Discussion

To verify the proposed scheme, simulation studies have been carried out for two-level, three-level, five-level and seven-level MPC inverter fed DTC IM Drive. The simulation parameters of induction motor used in this method are given as follows: $R_s=4.85\Omega$, $R_r=3.805\Omega$, $L_s=274\text{mH}$, $L_r=274\text{mH}$, $L_m=258\text{mH}$, $p=2$, $J=31\text{g.m}^2$, $V=220\text{V}$, power=1.5kW and speed=1420rpm. All Simulations have a sample time for the control loop of 100 μs ; the voltage of the DC bus is 514V.

Table 3: Proposed switching table for 7-Level MPC Inverter fed DTC IM drive.

		<i>Sectors</i>											
C_ϕ	C_Γ	1	2	3	4	5	6	7	8	9	10	11	12
-1	-6	304	314	305	316	300	306	301	308	302	310	303	312
	-5	224	234	225	236	220	226	221	228	222	230	223	232
	-4	104	114	105	116	100	106	101	108	102	110	103	112
	-3	67	83	68	85	63	75	64	77	65	79	66	81
	-2	117	209	118	210	113	205	114	206	125	207	116	208
	-1	5	48	6	49	1	44	2	45	3	46	4	47
	0	<i>Zero Vector</i>											
	+1	3	46	4	47	5	48	6	49	1	44	2	45
	+2	115	207	116	208	117	209	118	210	113	205	114	206
	+3	65	79	66	81	67	83	68	85	63	75	64	77
	+4	102	110	103	112	104	114	105	116	100	106	101	108
	+5	220	228	221	230	222	232	223	234	218	224	219	226
	+6	298	306	299	308	300	310	301	312	296	302	297	304
+1	-6	300	306	301	308	302	310	303	312	304	314	305	316
	-5	226	221	228	222	230	223	232	224	234	225	236	220
	-4	101	108	102	110	103	112	104	114	105	116	100	106
	-3	77	65	79	66	81	67	83	68	85	63	75	64
	-2	207	116	208	117	209	118	210	113	205	114	206	115
	-1	48	6	49	1	44	2	45	3	46	4	47	5
	0	<i>Zero Vector</i>											
	+1	45	3	46	4	47	5	48	6	49	1	44	2
	+2	208	117	209	118	210	113	205	114	206	115	207	116
	+3	67	84	68	86	63	76	64	78	65	80	66	82
	+4	115	105	117	100	107	101	109	102	111	103	113	104
	+5	223	235	218	225	219	227	220	229	221	231	222	233
	+6	313	296	303	297	305	298	307	299	309	300	311	301
0	-6	305	316	300	306	301	308	302	310	303	312	304	314
	-5	225	236	220	226	221	228	222	230	223	232	224	234
	-4	105	116	100	106	101	108	102	110	103	112	104	114
	-3	68	85	63	75	64	77	65	79	66	81	67	83
	-2	210	113	205	114	206	115	207	116	208	117	209	118
	-1	49	1	44	2	45	3	46	4	47	5	48	6
	0	<i>Zero Vector</i>											
	+1	44	2	45	3	46	4	47	5	48	6	49	1
	+2	205	114	206	115	207	116	208	117	209	118	210	113
	+3	76	64	78	65	80	66	82	67	84	68	86	63
	+4	107	101	109	102	111	103	113	104	115	105	117	100
	+5	225	219	227	220	229	221	231	222	233	223	235	218
	+6	303	297	305	298	307	299	309	300	311	301	313	296

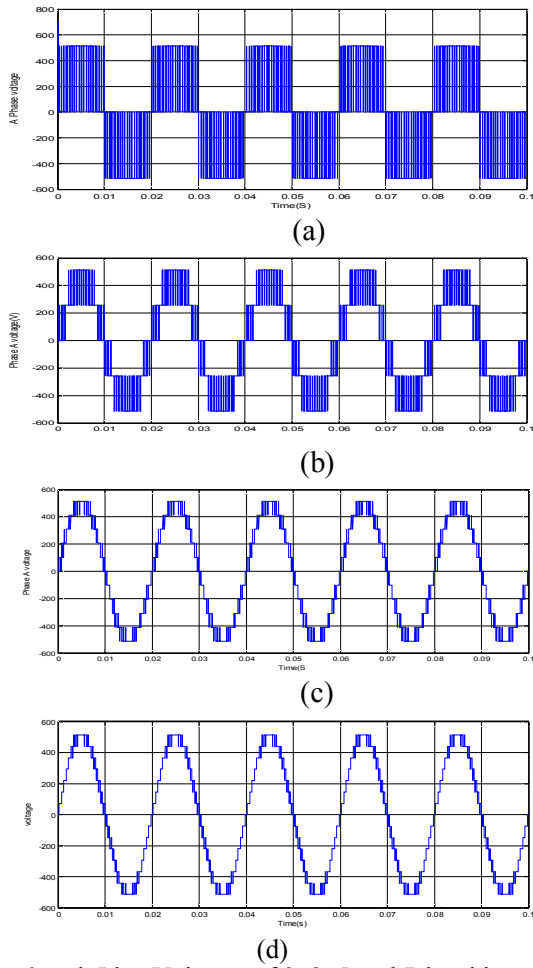


Fig.6: a-d: Line Voltages of 2, 3, 5 and 7-level inverter

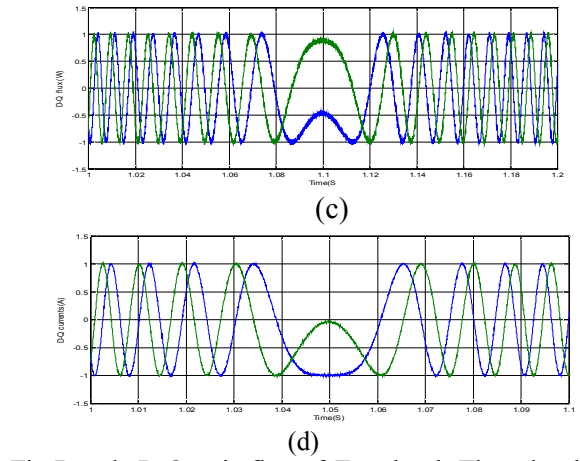
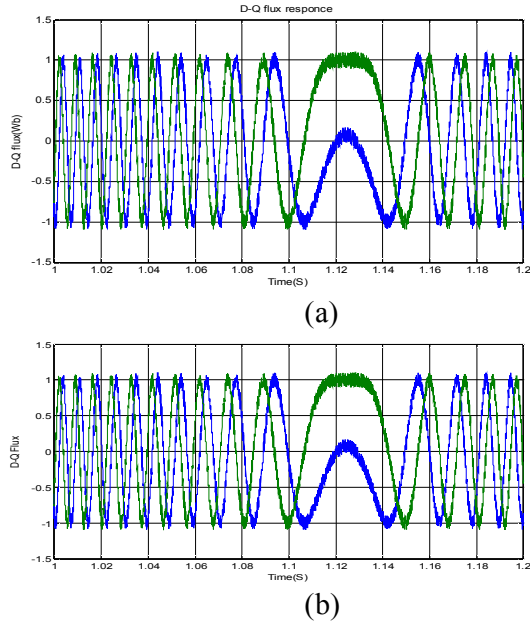


Fig.7: a-d D-Q axis flux of Two-level, Three-level , Five-level and Seven-level inverter fed DTC IM drive, current reversal at 1sec

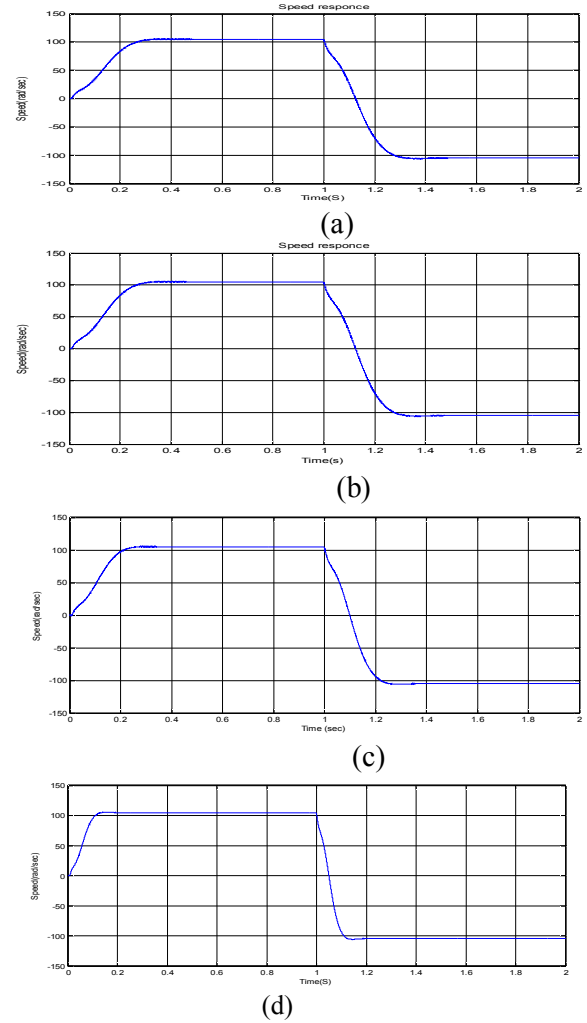


Fig.8: a-d Speed response of Two-level, Three-level , Five-level and Seven-level inverter fed DTC IM drive, current reversal at 1sec.

Table 4: Comparison between 2-level, 3-level, 5-level and 7-level MPC Inverter fed DTC IM drive

<i>Inverter fed DTC IM drive</i>	<i>Dynamic Speed recovery time (s)</i>	<i>Dynamic D-Q axis currents Recovery time(s)</i>	<i>Torque ripple magnitude(N-M)</i>	<i>%THD</i>
2-level	1.30	1.35	3.8	63.78
3-level	1.25	1.25	2.7	33.21
5-level	1.20	1.1	1.4	10.86
7-level	1.18	1.05	0.43	7.77

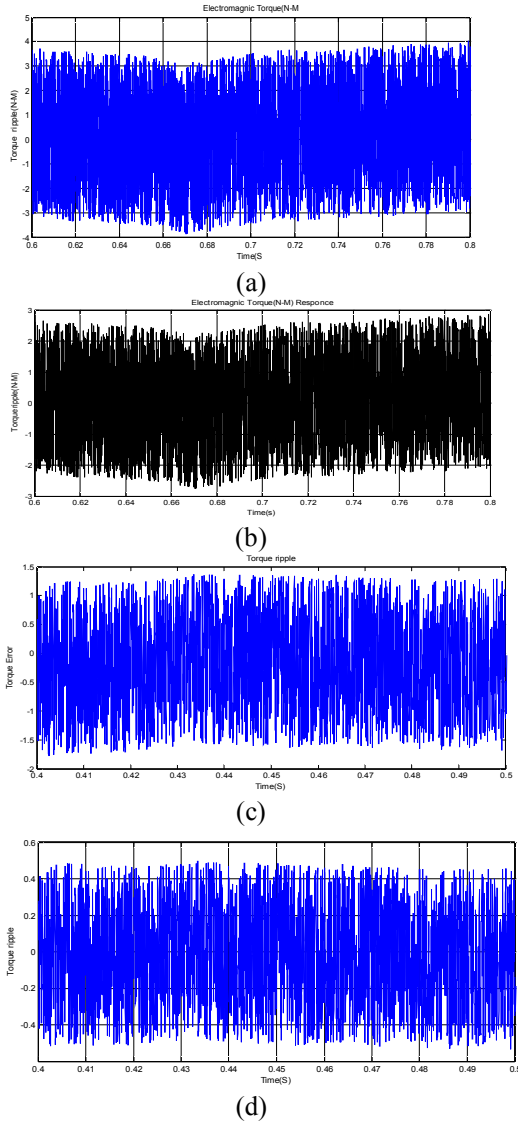


Fig.9: a-d Torque ripples magnitudes of Two-level, Three-level, Five-level and Seven-level inverter fed DTC IM drive, current reversal at 1sec.

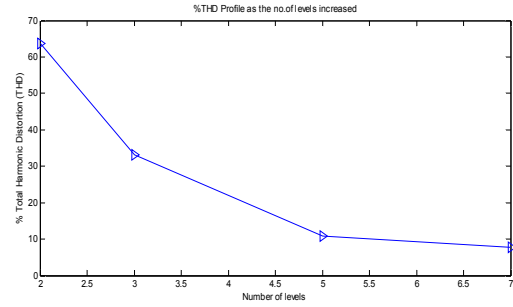


Fig.10: %THD profile as the number of levels increase

The stator line voltages of two-level, three-level, five-level and seven-level inverter system are illustrated in fig.6. In fig.7 D-Q axis flux response of the two-level, three-level five-level and seven-level inverters are compared. It is seen that the performance of the seven-level inverter fed DTC IM drive has lower ripple, so the proposed system is superior to control the flux with reduced ripple content. Fig. 8 illustrate the speed response of two-level, three-level, five-level and seven-level inverter fed DTC IM drive, from simulation results proposed system has fast dynamic speed response. Fig.9 shows the torque ripples magnitudes of two-level, three-level, five-level and seven-level inverter fed DTC IM drive ; demonstrates the proposed DTC's achieved high dynamic performance in response to changes in demand torque. Fig.10 shows the decrease of percentage of Total Harmonic Distortion (%THD) in the motor line voltage as the number of levels increased. This result in smooth running of motor and the performance of the motor can be improved.

From the above table 4 , the proposed DTC IM drive system behavior is optimum, even in extreme conditions like the reverse speed reference with nominal load torque applied. Reduction in ripple is observed in both electromagnetic torque and flux is due to the use of hysteresis controllers.

6. Conclusion

A multilevel inverter based DTC fed induction motor drive using space vector modulation is presented. The proposed DTC IM drive scheme is capable for enough degrees of freedom to control both electromagnetic torque and stator flux with very low ripple. Even with at the output voltages with extremely low distortion and lower dv/dt they can operate with a lower switching frequency. As the number of levels increased the %THD in the motor line voltage decreased. As the number of levels increased the torque ripple is reduced to minimum and the stator flux ripple is also minimized. From this analysis high dynamic performance, good stability and precision are achieved.

The proposed inverter scheme does not face any neutral-point fluctuations. Space vector modulation provides a more efficient use of the DC bus as well as smaller torque ripple, lower switching loss and a lower total harmonic distortion in an ac motor drive application.

From the simulation results, it can be concluded that the seven-level inverter fed DTC drive gives reduced steady state ripples and a harmonic distortion as the number of levels increased.

References

1. M. F. Escalante, J-C. Vannier and A. Arzandé. *Flying Capacitor Multilevel Inverters and DTC Motor Drive Applications*. IEEE Trans. On Industrial Electronics, vol. 49, (No.4), pp. 809-815, 2002.
2. J. Rodriguez, J-S Lai and F. Z. Peng. *Multilevel Inverters: A survey of topologies, controls, and applications*. IEEE Trans. On Industrial Electronics, vol. 49, (No.4), 2002.
3. Madhav D. Manjrekar and Thomas A. Lipo, *A Hybrid Multilevel Inverter Topology for Drive Application*, in Proceedings of the 1998 IEEE – APEC Conference, pp.523-529
4. A.Rufer, M.Veenstra and K.Gopakumar, *Asymmetric Multilevel Converter for High Resolution Voltage Phasor Generation*, in Proceedings of the 1999 EPE Conference, pp.P1-P10.
5. S. Busquets-Monge, S. Alepuz, J. Bordonau, and J. Peracaula, *Voltage balancing control of diode-clamped multilevel converters with passive front-ends*, IEEE Trans. Power Electron., vol. 23, no. 4, pp. 1751–1758, Jul. 2008.
6. Y. Zhang and Z. Zhao, *Study on capacitor voltage balance for multi-level inverter based on a fast SVM algorithm*. Proc. CSEE, vol. 26, no. 18, pp. 71–76, 2006, (in Chinese).
7. Dalessandro, S. D. Round, and J. W. Kolar, *Center-point voltage balancing of hysteresis current controlled three-level pwm rectifiers*, IEEE Trans. Power Electron., vol. 23, no. 5, pp. 2477–2488, Sep. 2008.
8. A. Nabae, I. Takahashi, and H. Akagi, *A new neutral-point clamped PWM inverter*, IEEE Trans. Ind. Appl., vol. IA-17, no. 5, pp. 518–523, Sep. 1981
9. J.-S. Lai and F. Z. Peng, *Multilevel converters—A new breed of power converters*, IEEE Trans. Ind. Applicat., vol. 32, pp. 509–517, May/June 1996.
10. B. McGrath, D. Holmes, T. Lipo. *Optimized Space Vector switching sequences for multilevel inverters*. IEEE Transactions on Power Electronics, 2003, 18(6): 1293–1301.
11. Z. Pan, F. Peng, et al. *Voltage balancing control of diode-clamped multilevel inverter system*, IEEE Transactions on Industry Applications, 2005, 41(6): 1698–1706.
12. J. Pou, D. Boroyevich, R. Pindado. *New Feed forward Space-Vector PWM Method to Obtain Balanced AC Output Voltages in a Three-Level Neutral-Point-Clamped Converter*. IEEE Transactions on Industrial Electronics, 2002, 49(5): 1026–1034.
13. J. Rodriguez, J. Lai, F. Peng. *Multilevel Inverters: A Survey of Topologies, Controls and Applications*. IEEE-IETrans. On Industrial Electronics, 2002, 49(4): 724–738.
14. P. Satish Kumar, J. Amarnath and S. V. L. Narasimham, *An Analytical Space-Vector PWM Method for Multi-Level Inverter Based on Two-Level Inverter*, International Review on Modelling and Simulations (IREMOS), Vol. 03, n.01, pp. 1-9, February 2010.
15. I. Takahashi and T. Nogushi. *A new quick-response and high efficiency control strategy of induction motor*. IEEE Trans. On. IA, vol. 22, (No.5), pp. 820-827, 1986.
16. G. Buja, D. Casadei and G. Serra. *Direct torque control of induction motor drives*. Proc. IEEE International Symposium on Industrial Electronics, vol. 1, pp. TU2-TU8, 1997.
17. P. Vas, *Sensor less Vector and Direct Torque Control*. Oxford, U.K.: Oxford Univ. Press, 1998.
18. D. Casadei, G. Grandi, G. Serra and A. Tani, *Switching strategies in direct torque control of induction machines*, ICEM 94, Vol. 2, pp. 204-209, 1994.
19. I. Messaif, E.M. Berkouk, N. Saadia and A. Talha, *Application of Direct Torque Control Scheme for Induction Motor*, International AMSE Conference MS05, 2005.
20. Messaif, E.M. Berkouk, N. Saadia, *An Improved DTC strategy for induction machine control fed by a multilevel voltage source inverter*, IEEE International Conference on Electronics, Circuits and Systems, Morocco.
21. O. Chandrasekhar, K. Chandra sekhar, “*Five-level SVM Inverter for an Induction motor with Direct Torque Controller*” Journal of Electrical Engineering, vol.13/2013- Edition:4, pp.53-61
22. O. Chandra sekhar, K. Chandra sekhar “*Multilevel Inverter Fed DTC Control of Induction Motor Drive*” International review of modeling and simulation (IREMOS), Vol.5, N.6, pp:146 -153, Feb.2012
23. O. Chandra Sekhar and Dr.K. Chandra Sekhar “*A Novel Five-level inverter Topology for DTC Induction Motor Drive*” 2012 IEEE International Conference on Advanced Communication Control and Computing Technologies, Proceeding of IEEE-ICACCCT, 2012, pp.375-379